RADIAL CONSOLIDATION ANALYSIS USING DELAYED CONSOLIDATION APPROACH

PANKAJ BARAL

PhD, MEng (AIT), BEng (Civil), MIEAust

Associate Research Fellow, Centre for Geomechanics and Railway Engineering,

School of Civil Engineering, Faculty of Engineering and Information Sciences,

University of Wollongong, Wollongong City, NSW 2522, Australia

CHOLACHAT RUJIKIATKAMJORN

PhD, MEng (AIT), BEng (Hons), FIEAust, MASCE

Associate Professor, Centre for Geomechanics and Railway Engineering,

University of Wollongong, Wollongong City, NSW 2522, Australia

BUDDHIMA INDRARATNA

PhD (Alberta), MSc (Lond.), BSc (Hons., Lond.), FTSE, FIEAust., FASCE, FGS, DIC

Distinguished Professor of Civil Engineering, Faculty of Engineering;

Director, Centre for Geomechanics and Railway Engineering;

University of Wollongong, Wollongong City, NSW 2522, Australia

SERGE LEROUEIL

Professor, Department of Civil Engineering, Laval University, Quebec City, QC, Canada

JIAN-HUA YIN

Chair Professor of Soil Mechanics, Department of Civil and Environmental Engineering, The Hong Kong Polytechnic University, Hung Hom, Kowloon, Hong Kong

Submitted to: Journal of Geotechnical and Geoenvironmental Engineering, ASCE

Author for correspondence:
Prof. B. Indraratna
Faculty of Engineering
University of Wollongong
Wollongong, NSW 2522
Australia.
Ph: +61 2 4221 3046
Fax: +61 2 4221 3238
Email: indra@uow.edu.au

RADIAL CONSOLIDATION ANALYSIS USING DELAYED CONSOLIDATION APPROACH

Pankaj Baral[1], Cholachat Rujikiatkamjorn[2], Buddhima Indraratna[3*], Serge Leroueil[4] & Jian-Hua Yin[5]

[1]Associate Research Fellow, Centre for Geomechanics and Railway Engineering, School of Civil Engineering, Faculty of Engineering and Information Sciences, University of Wollongong, Wollongong City, NSW 2522, Australia

[2]Associate Professor, Centre for Geomechanics and Railway Engineering, University of Wollongong, Wollongong City, NSW 2522, Australia

[3*]Distinguished Professor of Civil Engineering, Faculty of Engineering; Director, Centre for Geomechanics and Railway Engineering; University of Wollongong, Wollongong City, NSW 2522, Australia (Corresponding Email Address: indra@uow.edu.au)

[4]Professor, Department of Civil Engineering, Laval University, Quebec City, QC, Canada

[5]Chair Professor of Soil Mechanics, Department of Civil and Environmental Engineering, The Hong Kong Polytechnic University, Hung Hom, Kowloon, Hong Kong.

ABSTRACT: The paper is an analytical solution for radial consolidation that captures isotaches with a strain rate dependency of pre-consolidation pressure. These relationships are obtained based on Constant Rate of Strain (CRS) and long-term consolidation (LTC) tests, and then used in the radial consolidation model incorporating the field strain rate which is generally much lower compared to the typical laboratory environment. In this study the calculated settlement and associated excess pore water pressure are obtained using the equivalent pre-consolidation pressure from the reference isotache, within the $(\frac{\sigma_p{}'}{\sigma_{p0}{}'})$ - $(\dot{\varepsilon_v})$ domain. Moreover, the change in $\frac{C_\alpha}{C_c}$ ratio (i.e. secondary compression index / compression index) with decreasing strain rate is used to calculate the long term settlement. This method is then validated using various case histories in Australia and Southeast Asia, where excess pore water pressure is dissipated at a slower rate in relation to the observed settlement.

KEYWORDS: Radial consolidation, isotaches, viscosity, creep settlement

65 ## 1. INTRODUCTION

66 Many coastal regions of Australia and Southeast Asia consist of very soft clays (estuarine or
67 marine) which contain adverse geotechnical properties such as low bearing capacity and
68 excessive settlement. These properties present challenges in design and construction,
69 especially minimising long term deformation over the lifetime of the infrastructure. The
70 construction, design, and stability of transport infrastructure are of global economic
71 significance, particularly along coastal regions where many nations spend millions of dollars
72 annually on road maintenance alone. In Australia, this is why improving the geotechnical
73 properties of saturated soft clays of significant depths (say 20 m) and being able to accurately
74 predict the long term deformation have significant benefits to both urban and regional
75 communities where much transport infrastructure is currently being developed.

76 The use of PVD combined with either surcharge or vacuum preloading could reduce the
77 construction and maintenance costs significantly and also enhance the performance of
78 infrastructure through better drainage, greater load bearing capacity, and reduced long term
79 settlement of the improved soil. The advantages of PVDs alone have been vividly elucidated
80 elsewhere by Holtz et al. (1991). The preloading method of stabilising soft clays by surcharge
81 fill embankments (facilitated by PVDs) is generally a low-cost solution (Hansbo 1981,
82 Bergado et al. 1991, Almeida et al. 2000). However, in sites with thick soft soil,
83 consolidation is gradual due to the very low permeability of the soil and its inherent
84 thickness. The installation of PVDs can facilitate rapid excess pore pressure dissipation in
85 soft soil foundation when raising a surcharge embankment (Kjellman 1952; Bergado et al.
86 2002; Bo et al. 2003; Geng et al. 2012). When such a system is combined with vacuum
87 preloading even faster rate of dissipation can be achieved with an enhanced rate of settlement
88 especially at the start, thereby enabling the final settlement to be approached within a shorter
89 period of time (Chu & Yan 2005; Indraratna et al. 2005).

Analytical solutions for radial consolidation have been developed to consider various aspects such as the smear zone, stratified soils, and vacuum preloading (Barron, 1948; Tang and Onitsuka, 2001; Indraratna et al. 2005; Walker and Indraratna, 2009), however, limited efforts have been made to analytically incorporate the effect of soil viscosity as influenced by the strain rate (Yang et al. 2016). Indraratna et al. (2018) developed a radial consolidation model considering elastic visco-plastic properties of soft soil and validated using prediction embankment at Ballina confirming visco-plastic model's accuracy compared with other method of prediction. Evaluating the time-dependent behaviour of soft soils is crucial for predicting the correct settlement and excess pore water. Two different methods (Hypotheses A and B, see Fig. 1) have been considered herein to evaluate the long term time-dependent settlement as below:

Hypothesis A: Creep deformation is assumed to occur after the excess pore water has completely dissipated and the ratio (C_α/C_c) between the coefficient of secondary consolidation (C_α) and (C_c), is assumed to be constant. Strain occurs during primary consolidation as the excess pore water pressure dissipates, and strain also occurs during secondary consolidation (Ladd, 1973; Mesri and Castro, 1987). The coefficient of secondary consolidation (C_α) is used to estimate the resulting viscous deformations. Although Hypothesis A is simple and often used due to the availability of C_α and C_c, this approach can result in continuous long term settlement even at an infinite time.

***Hypothesis B*:** The concept of isotache (Sulkje 1957; Barden 1969; Bjerrum 1967) assumes that some structural viscosity is responsible for creep that begins during the primary consolidation phase as the excess pore water pressure dissipates (Fig. 1). Strain during primary consolidation depends on the thickness of the sample and the strain rate; this is why the experimental results obtained from relatively thin samples may not correctly represent the actual in-situ behaviour of thick clay deposits due to the obvious implications of a different

time scale. In this hypothesis a series of compression curves are used to show the relationship between the strain rate and pre consolidation pressure (Fig. 2). The creep ratio (i.e. $C_{\alpha e}/C_c$) decreases with the strain rate that diminishes with time. Various studies have already been carried out on Hypothesis B (e.g. Leroueil et al., 1988; Adachi et al., 1996 and Kim and Leroueil, 2001).

Specific studies considered the time-dependent behaviour of soft soil using the Isotache concept in conjunction with the strain rate dependency of pre-consolidation pressure (Watabe and Leroueil, 2015 and Tanaka, 2006). These isotaches are normally characterised by a reference compression line obtained from a constant rate of strain (CRS) test and a series of long term consolidation tests. Tsusumi and Tanaka (2011) designed a special CRS test and carried out testing on a single sample with a multiple strain rate applied at different stages. In this study the isotache concept is incorporated into the radial consolidation model to predict the actual field performance in terms of settlement and the associated dissipation of excess pore water.

2. ANALYTICAL MODEL FOR RADIAL CONSOLIDATION INCORPORATING THE ISOTACHE CONCEPT

Based on the unique relationship between the strain and pre-consolidation pressure which corresponds to the strain rate model proposed by Watabe and Leroueil (2015), a strain rate dependency relationship with pre-consolidation pressure can be established using long term consolidation (LTC) and a constant rate of strain (CRS) test (Fig. 2). The upper bound of the isotache represents the compression curve in the laboratory experiment with a higher strain rate whereas other isotache lines resemble compression curves at lower strain rates. The relationship between pre-consolidation pressure and strain rate can be expressed as:

$$\sigma_p' = f(\dot{\epsilon_v}) \quad (1)$$

In the above, the exponential relationship between the pre-consolidation pressure and the strain rate can be determined by using two expressions (Kobayashi et al. 2005).

$$\ln \sigma_p' = a_1 + a_2 \ln \dot{\epsilon_v} \quad (2)$$

The first expression is expressed by Eq (2), where the relationship between $\ln \sigma_p'$ and $\ln \dot{\epsilon_v}$ is linear, the model may seem unrealistic as σ_p' becomes zero when $\dot{\epsilon_v}$ decreases to zero. Therefore, a second expression (i.e. Eq 3) has been proposed to remediate this condition, where σ_{pL}' is introduced as a lower limit of σ_p' so when $\dot{\epsilon_v}$ decreases to zero in Eq (3), σ_p' converges to σ_{pL}'.

$$\sigma_p' = \sigma_{pL}' + b_1 \exp(b_2 \ln \dot{\epsilon_v}) \quad (3)$$

The exponential form Eq (3) can be shown to yield Eq (4) in logarithmic form:

$$\ln \frac{\sigma_p' - \sigma_{pL}'}{\sigma_{pL}'} = c_1 + c_2 \ln \dot{\epsilon_v} \quad (4)$$

$$\dot{\epsilon_v} = \left(\frac{\sigma_p' - \sigma_{pL}'}{\sigma_{pL}'}\right)^{\frac{1}{c_2}} \; exp^{-\frac{c_1}{c_2}} \quad (5)$$

$$\dot{\epsilon_v} = c_3 \left(\frac{\sigma_p' - \sigma_{pL}'}{\sigma_{pL}'}\right)^{c_4} \quad (6)$$

where $\sigma_p' = preconsolidation\ pressure\ at\ a\ given\ strain\ rate$,

a_1, a_2, b_1 & b_2 are empirical constants during the derivation

$\sigma_{pL}' = lower\ limit\ of preconsolidation\ pressure$,

141 $\epsilon_v^{\cdot} = \ axial\ strain\ rate$

142 $c_3 = \ exp^{-\frac{c_1}{c_2}}$ and $c_4 = \frac{1}{c_2}$ are two constants used in the model

143 $c_1 = \ln\frac{{\sigma_p}' - {\sigma_{pL}}'}{{\sigma_{pL}}'}\ at\ \epsilon_v^{\cdot} = 1 \times 10^{-7} s^{-1}$ and $c_2 = \frac{1}{\ln \dot{\epsilon_v}}\left[\ln\frac{{\sigma_p}' - {\sigma_{pL}}'}{{\sigma_{pL}}'} - c_1\right]$

144 The lower limit of pre consolidation pressure (${\sigma_{pL}}'$) can be calculated based on Eq. (6). The
145 illustration of the above mentioned procedure to evaluate how the strain rate depends on the
146 pre-consolidation pressure (${\sigma_p}'$) from the CRS and LTC test is shown in Fig. 2. This analysis
147 was carried out using clay samples obtained from Ballina, Australia. Please note that ${\sigma_{p0}}'$ is
148 the value of preconsolidation pressure when strain rate is $1 \times 10^{-7} s^{-1}$, which is close to the
149 average strain rate obtained in 24-h incremental loading consolidation tests.

150 The normalised relationship in between the $(\frac{{\sigma_p}'}{{\sigma_{p0}}'})$- $(\dot{\varepsilon_v})$ for an array of worldwide clays has
151 already been examined and provided by Watabe et al. (2012) and Leroueil (1988). The
152 relationship also captures clays obtained from Ballina, Bangkok (Rujikiatkamjorn et al.,
153 2008), Malaysia (Indraratna and Redana, 2000) and Singapore (Cao et al., 2001) but with
154 different coefficients for specific type of soil (Fig. 3). The ratio $\frac{{\sigma_{pL}}'}{{\sigma_{p0}}'}$ for Ballina clay is 0.86
155 and $\frac{{\sigma_p}'}{{\sigma_{p0}}'}$ approaches unity at $\dot{\varepsilon} = 1 \times 10^{-07} s^{-1}$; for Ballina clay the value of c_3 and c_4 are
156 3.63×10^{-3} and 6.33, respectively (Fig. 3).

157 Figure 4 shows a soil with a pre-consolidation pressure (${\sigma_p}'$) of soil that has been loaded
158 from an initial effective stress of ${\sigma'}_{v0}$ to the final effective stress ${\sigma'}_{vf}$ in the laboratory
159 environment and therefore the corresponding strain rate for the sample is $\dot{\varepsilon}_1$. For a given
160 preloading ($\Delta\sigma_t$), the change in effective stress can be calculated by:

$$\Delta\sigma_t' = \Delta\sigma_c' + \Delta\sigma_d' \quad (7)$$

The first term $\Delta\sigma_c'$ is an increase in effective stress due to the dissipation of excess pore-water whereas the second term ($\Delta\sigma_d'$) is an increase in effective stress due to delayed consolidation caused by the viscosity of clay. In order to estimate $\Delta\sigma_d'$, the strain rate dependency of preconsolidation pressure can be employed using the following relationship:

$$\Delta\sigma_d' = \sigma_{p0}' - \sigma_{p(\dot{\varepsilon})}' \quad (8)$$

where σ_{p0}' corresponds to the laboratory pre-consolidation pressure which corresponds to a strain rate of $1 \times 10^{-07} s^{-1}$, and $\sigma_{p(\dot{\varepsilon})}'$ is the preconsolidation pressure at a given strain rate ($\dot{\varepsilon}$). It should be noted that the strain rate can affect the location of $\sigma_{p(\dot{\varepsilon})}'$in isotaches. The strain rate can be estimated using the following formulation:

$$\dot{\varepsilon} = \frac{\varepsilon_{U100}}{\Delta t_{U100}} \quad (9)$$

where $\varepsilon_{U100}\ and\ \Delta t_{U100}$ are the strain and time at the degree of consolidation based on pore pressure equal to 100% (U_{100}) respectively; these parameters can be calculated based on the formulations proposed earlier by Indraratna et al. (2005), so once the strain rate ($\dot{\varepsilon}$) is known, $\sigma_{p(\dot{\varepsilon})}'$ can be calculated using Equation (6).

After estimating $\Delta\sigma_d'$ using Eq. (8), the term σ'_{vc} can be calculated from the following equation:

$$\sigma'_{vc} = \sigma'_{vf} - \Delta\sigma_d' \quad (10)$$

Here the term σ'_{vc} represents the corresponding value of effective stress on x-axis after considering delayed consolidation. Once σ'_{vc} has been calculated, the dissipation of excess

pore water pressure and consolidation settlement (δ_c) can then be determined using the formulations as elaborated below:

Indraratna et al. (2005) proposed an analytical solution to capture the nonlinear compressibility and permeability of soil, so the excess pore pressure at a radial distance r from the centre of drain at any time t (u_r) while considering the linear variation of permeability in the smear zone, can be calculated by:

$$u_r = \frac{1}{\mu {r_e}^2}\left[{r_e}^2 \ln\left(\frac{r}{r_w}\right) - \frac{(r^2 - {r_w}^2)}{2}\right] exp\left(-\frac{8{T_{h0}}^*}{\mu}\right)\Delta\sigma_t; \quad \sigma_v{}' \leq \sigma_{p(\dot{\varepsilon})}{}' \text{ and } t \leq t_i \tag{11a}$$

$$u_r = \frac{1}{\mu {r_e}^2}\left[{r_e}^2 \ln\left(\frac{r}{r_w}\right) - \frac{(r^2 - {r_w}^2)}{2}\right] exp\left(-\frac{8{T_{hi}}^*}{\mu}\right)\left(\sigma'_{v0} + \Delta\sigma_t - \sigma_{p(\dot{\varepsilon})}{}'\right) \; ; \; u_r = \sigma'_{v0} + \Delta\sigma_t - \sigma_{p(\dot{\varepsilon})}{}' \text{ at } T_{hi} = 0 \text{ and } t = t_i, \text{ for } \sigma_v{}' > \sigma_{p(\dot{\varepsilon})}{}' \text{ and } t > t_i, \tag{11b}$$

where $\mu = ln\left(\frac{n}{s}\right) - \frac{3}{4} + \frac{\kappa(s-1)}{s-\kappa} ln\left(\frac{s}{\kappa}\right)$, $n = \frac{r_e}{r_w}$ and $s = \frac{r_s}{r_w}$

In the above expressions, r_w is the radius of the drain and r_e is the equivalent diameter of the soil cylinder which is a function of drain spacing. Similarly, r_s is the radius of the smear zone and κ is the permeability index.

The modified time factor ${T_h}^*$ for radial consolidation with a vertical drain that includes the smear effect can be expressed by the following relationships:

When $\sigma_v{}' \leq \sigma_{p(\dot{\varepsilon})}{}'$ and $t \leq t_i$

$${T_{h0}}^* = P_{av,0}T_{h0} = 0.5\left[\left(\frac{\sigma_{p(\dot{\varepsilon})}{}'}{\sigma'_{v0}}\right)^{1-\left({c_r}/{c_k}\right)} + 1\right]T_{h0} \tag{12a}$$

$$P_{av,0} = 0.5\left[\left(\frac{{\sigma_{p(\dot{\varepsilon})}}'}{\sigma'_{v0}}\right)^{1-\left(c_r/c_k\right)} + 1\right] \quad (12b)$$

When ${\sigma_v}' > {\sigma_{p(\dot{\varepsilon})}}'$ and $t > t_i$

$$T_{hi}{}^{*} = P_{av,i}T_{hi} = 0.5\left[\left(\frac{\sigma'_{v0} + {\Delta\sigma_t}'}{{\sigma_{p(\dot{\varepsilon})}}'}\right)^{1-\left(c_c/c_k\right)} + 1\right]T_{hi} \quad (12c)$$

$$P_{av,i} = 0.5\left[\left(\frac{\sigma'_{v0} + {\Delta\sigma_t}'}{{\sigma_{p(\dot{\varepsilon})}}'}\right)^{1-\left(c_c/c_k\right)} + 1\right] \quad (12d)$$

$P_{av,0}$ & $P_{av,i}$ used in the above equations are the factors used to convert dimensionless time factors (T_{h0} & T_{hi}) into their modified form ($T_{h0}{}^{*}$ & $T_{hi}{}^{*}$). Now the ratio (R_u) for the dissipation of excess pore pressure at a distance r from the centre of the drain at a given time t, can be calculated as:

$$R_u = \frac{u_r - {\Delta\sigma_d}'}{\Delta\sigma_t - {\Delta\sigma_d}'} \quad (13)$$

Similarly, the consolidation settlement (δ_c) can be calculated using the following formulation:

$$\delta_c = \frac{Hc_r}{(1+e_0)}\log\left(\frac{{\sigma_v}'}{{\sigma'}_{v0}}\right) \qquad \text{for } {\sigma_v}' \le {\sigma_{p(\dot{\varepsilon})}}' \quad (14a)$$

$$\delta_c = \frac{H}{(1+e_0)}\left[c_r\log\left(\frac{{\sigma_{p(\dot{\varepsilon})}}'}{{\sigma'}_{v0}}\right) + c_c\log\left(\frac{{\sigma'}_{vc}}{{\sigma_{p(\dot{\varepsilon})}}'}\right)\right] \qquad \text{for } {\sigma_v}' > {\sigma_{p(\dot{\varepsilon})}}' \quad (14b)$$

where c_c = compression index, c_r = recompression index, and H = compressible soil thickness.

The total settlement (δ_t) consists of consolidation settlement due to the dissipation of excess pore pressure (δ_c) and delayed settlement (δ_a) which is calculated by using the variation of secondary consolidation coefficient with the strain rate as shown in Fig. 5(b).

$$\delta_t = \delta_c + \delta_a \tag{15}$$

The degree of consolidation (DOC) based on the settlement DOC_{sett} and the excess pore water pressure (EPWP), means that DOC_{EPWP} can be now determined by:

$$DOC_{sett} = \left(\frac{\delta_t}{\delta_{ult}}\right) \times 100 \tag{16}$$

and

$$DOC_{EPWP} = \left(\frac{u_0 - u_t}{u_0 - \Delta\sigma_d{}'}\right) \times 100 \tag{17}$$

where $\delta_t \; and \; \delta_{ult}$ represent settlement at any time and ultimate settlement, whereas $u_0 \; and \; u_t$ represent the initial excess pore water pressure to be dissipated and excess pore water pressure at a given time t, respectively.

The slope (α) of the log ($\frac{\sigma_p{}'}{\sigma_{p0}{}'}$)-log ($\dot{\varepsilon}$) at a given strain rate is equal to the secondary compression index (c_α) and the compression index (c_c), and is given by the following relationship:

$$\alpha = \frac{\Delta \log\left(\frac{\sigma_p{}'}{\sigma_{p0}{}'}\right)}{\Delta \log(\dot{\varepsilon})} = \frac{c_\alpha}{c_c} \tag{18}$$

Mesri and Castro (1987) proposed a constant ratio (c_α/c_c) for clay and stated that this value was 0.04±0.01 for inorganic clays. However, according to Watabe and co-workers (Watabe & Leroueil, 2015 , and Watabe et al. 2008), the latter is not constant because the ratio of c_α/c_c decreases as the strain rate decreases. Figure 5 (a) shows the strain rate dependency of pre-

consolidation pressure for Ballina clay with a constant slope (i.e. 0.047), whereas Figure 5 (b) shows that the ratio α (c_α/c_c) decreases as the strain rate decreases. The value proposed by Mesri and his co-workers is typically valid for a laboratory strain rate range of 1×10^{-4} s^{-1} to 1×10^{-6} s^{-1} (see Fig. 5b). These results confirm the observations made by Leroueil (2006) for Canadian and Swedish clays as well as those by Watabe et al. (2012) for other clays. Based on variations of c_α/c_c ratio with the strain rate, a delayed settlement can be calculated.

3. PARAMETRIC STUDY ON THE INFLUENCE OF THE LENGTH OF DRAINAGE PATH

A parametric study has been carried out on specimens with three different equivalent diameters (D_e), Sample A: (75mm laboratory Rowe cell), Sample B: 350mm (large-scale sample) and Sample C: 1356 mm (representing vertical drain installed at 1.2 m spacing in a square pattern), with the consolidation of the 75 mm diameter specimen noted as to determine a isotache. The drain and soil parameters are listed in Table 1. The strain rates for Samples A, B and C are approximately 1.86×10^{-7}, 1.97×10^{-8} and 2.01×10^{-9} s^{-1}, respectively. From Eq. (6), the pre-consolidation pressures are 44.05, 41.84 and 39.64 kPa for Samples A, B and C, respectively.

The strain calculated from Eq. 14(a) and Eq. 14(b) and the excess pore water pressures calculated from Eq. 11(a) and 11(b) are shown in Figures 6(a) and 6(b), respectively. Note that sample A with a shorter drainage path experiences more creep settlement at the end of consolidation than sample B and sample C (Fig. 6a). This can be attributed to the additional settlement (δ_a) calculation for sample A when the strain rate changes from $1.86\times10^{-7}s^{-1}$ to 2.01×10^{-9} s^{-1}. Similarly, as the pre-consolidation pressure changes from 44.05 (sample A) to 41.84 (sample B) and 39.64 kPa (sample C), the increases in effective stress due to delayed

236 consolidation ($\Delta\sigma_d{}'$) are (0, 2.20 & 4.40 kPa), resulting in undissipated EPWP at the end of
237 consolidation (Figure 6b). The corresponding degree of consolidation based on settlement
238 and excess pore water pressure (EPWP) are then calculated using Eqs. (17) and (18) and are
239 shown in Fig. 6(c). Note that the degree of consolidation obtained from settlement always
240 overpredicts the degree of consolidation from EPWP; this is a typical occurrence most case
241 histories worldwide (Chu and Yan, 2005).

242 4. APPLICATION TO CASE HISTORIES

243 The application of the proposed model is demonstrated, for selected sites at the Pacific
244 Highway, Ballina, Australia, the Second Bangkok International Airport in Thailand, and
245 Muar clay in Malaysia. The settlement and excess pore water pressure predicted at the
246 centrelines of the embankments are compared to the field data.

247 4.1 Pacific Highway, Ballina, Australia

248 This site has a trial embankment built on uniform layers of soft to firm estuarine and alluvial
249 clays above residual soil and bedrock. The soft clay beneath the embankment is 25 m thick,
250 and the basic properties of the clay (water content, density, void ratio and the soil profile) are
251 shown in Figure 7 (Indraratna et al., 2012). The groundwater table is located 0.2 m below the
252 ground, and it consists of 10 m thick, soft silty clay with undrained shear strength of 5-15
253 kPa, followed by medium silty clay to a depth of 25 m with maximum undrained shear
254 strength of 48 kPa.

255 According to Kelly and Wong (2009), a total surcharge thickness of up to 11.2m, depending
256 on the thickness of the clay, has been selected to limit post-construction settlement to 50 mm
257 assuming soil density of 20 kN/m^3. To accelerate consolidation, circular vertical drains (34
258 mm diameter) were installed 1m apart in a square grid. In two sections of the embankment,

Section B was consolidated with vacuum and surcharge preloading, which further reduced the construction time. Section A was consolidated with conventional fill surcharge. At section A, the surface settlement obtained from settlement plate (SP1) and excess pore pressure obtained from the piezometer (P1) installed 3.3 m deep at the embankment centreline is used for the purpose of comparison. The embankment was raised to a height of 2 m within 150 days, and then to 4 m high after 250 days. Table 2 tabulates the drain properties with the diameter of the smeared zone and the ratio of pre-consolidation pressure ($\frac{\sigma_{pL}'}{\sigma_{p0}'}$) with two other parameters (c_3 & c_4), as defined in Eq (6). The properties of Ballina clay with corresponding pre-consolidation pressure are presented in Table 3 (Indraratna et al. 2012)

The staged loading, field time-settlement, and EPWP dissipation curves with predictions using the current model, Yin and Graham (1989), as well as the finite element analysis using converted permeability by Indraratna and Redana (2000) are plotted in Fig 8. An average field strain rate of 8.54×10^{-11} s^{-1} is determined using Eq. (9), and it is significantly lower than the laboratory strain rate (1×10^{-07} s^{-1}). The settlement curve obtained from the current model always overpredicts two other curves as it accounts for creep using the variation of coefficient of secondary consolidation with a decreasing strain rate. However, the settlement predicted from all three models still provides an acceptable agreement with the field data. The recorded EPWP before 100 days is not available (Fig. 8c), but the EPWP dissipation curve based on the current isotache model is in closer agreement with the field data after incorporating delayed consolidation. The current model shows the retardation of excess pore water pressure dissipation and the value of EPWP remains at 32 kPa even after 445 days, whereas it decreases to 20 and 12 kPa based on the models proposed by Yin and Graham (1989) and Indraratna and Redana (2000).

4.2 Second Bangkok International Airport (SBIA), Thailand

283 The Second Bangkok international airport (AIT, 1995) was built on swampy land with
284 marine deposits. Ground level was located almost 1m above the mean sea level. The site
285 consisted of about 1.5 m thick weathered crust above 12m of soft clay followed by 8-10 m of
286 stiff clay followed by a uniform layer of dense sand.

287 For the soil strata, Figure 9 shows the water content (w), Atterberg limits (LL, PL, PI), unit
288 weight (γ), and specific gravity (G_s) with depth. The shear strength of clay at different depths
289 and corresponding compressibility parameters are shown in Fig. 10. Note that the shear
290 strength of the upper weathered crust was in the range of 30-40 kPa, but that of the
291 underlying soft soil to a depth of 9 m was relatively low (5-10 kPa).

292 Prefabricated vertical drains were installed to a depth of 12m to increase the shear strength
293 and reduce long term deformation. A cross section of the embankment and the layout of PVD
294 for Section TS2 is shown in Fig. 11. PVDs (94 mm by 3 mm) with grooved channels (made
295 up of Polyolefin) were installed with a 125 mm × 45 mm rectangular mandrel. The drains
296 were set 1.2 m apart in a square pattern. The surcharge fill (4.2m high) was completed in four
297 different stages within 275 days (see Figure 11a).

298 Table 4 lists the properties of the drains and strain dependency parameters. The field strain
299 rate was estimated to be 1.22×10^{-12} s^{-1}. A pre-consolidation pressure ratio of 0.82 and the
300 necessary parameters (c_3 & c_4) based on Fig. 3 are also shown in Table 4, and Table 5 shows
301 the soil properties which correspond to different layers together with the associated pre-
302 consolidation pressure.

303 The stage loading with time surface settlement and excess pore pressure at 2m deep curves
304 are plotted together with the predictions in Fig. 12. Note here that, as with previous case
305 histories, the settlement predictions using all three models are generally in a good agreement
306 with the field data. The remaining excess PWPs to be dissipated at the end of 420 days are

307 4.40, 2.60 & 1.30 kPa for the current model, Yin and Graham (1989) and Indraratna and
308 Redana (2000), respectively. The excess pore water pressure dissipation from the proposed
309 model improves significantly and agrees well with field observation when strain rate
310 dependency of pre-consolidation pressure is taken into account along with isotache approach.
311 Additional analyses (see Fig. 13) were conducted using subsurface settlements at 2, 8 and 12
312 m deep and it is found that the measured settlements at different depths can be accurately
313 predicted using this model. The comparisons of EPWP at the similar depths were excluded
314 due to the lack of field EPWP data.

315 **4.3 Muar clay, Malaysia**

316 The Malaysian Highway Authority chose a variety of ground improvement techniques at
317 Muar plain along the North South Expressway, to avoid excessive differential settlement
318 (Ratnayake, 1991). The techniques applied in the field consisted of electro osmosis, chemical
319 injection, micro piles, sand compaction piles, pre- stressed spun piles, well point preloading,
320 vacuum preloading, and sand wick installation and preloading with drains. These methods
321 were tested on Muar clay at 14 different sites, most of which consisted of marine and deltaic
322 origin with thick, problematic soft soil. In this paper, the section with conventional surcharge
323 preloading was used for the purpose of comparison.

324 This Muar clay consisted of 2 m of weathered crust above 16m thick soft to very soft silty
325 clay followed by 1m thick organic clay; it also contained medium dense to dense clayey silty
326 sand below the organic clay which extended up to 24 m from the ground surface. The
327 weathered clay was slightly over-consolidated compared to normally consolidated soft clay.
328 The water content and the Atterberg limits of soil, the over-consolidation ratio (OCR),
329 compressibility parameters with layer classification are shown in Fig. 14. The unit weight of
330 soft clay was almost uniform (15-16 kN/m^3) except for the top weathered crust which is

331 17kN/m^3. The undrained shear strength of the sample located at a depth of 3 m was 8 kPa,
332 and it increased linearly with depth. Several in-situ and laboratory experiments were also
333 carried out to obtain the soil parameters required for the analysis.

334 An embankment (4.74m high) was constructed above the soft soil in two stages. In the first
335 stage the embankment was raised to a height of 2.57m, and then fill was added until it
336 reached a height of 4.74 m. Band drains (r_w=0.035 m) were then installed in a triangular
337 pattern at 1.3 m spacing to a depth of 18 m. Settlement plates, piezometers and inclinometers
338 were then installed to monitor the embankment. A cross-section of this embankment
339 stabilised with PVDs showing the layout of the instrumentation is shown in Fig. 15.

340 The average field strain rate is calculated as 6.78×10^{-11} s^{-1} based on which a ratio of field pre-
341 consolidation pressure / laboratory pre-consolidation pressure equals to 0.79. These
342 parameters were used to calculate the current model. Table 6 provides the drain and strain
343 rate dependency ratio to convert the laboratory pre-consolidation pressure into the field pre-
344 consolidation pressure. Table 7 presents the parameters for the sub-soil layer with
345 corresponding pre-consolidation pressures. Figure 16 shows the staged construction, time
346 surface settlement curve, and EPWP dissipation at 3m deep pattern of Muar clay of the
347 current isotache model in comparison with the earlier models by Yin and Graham (1989) and
348 Indraratna and Redana (2000). The settlement predicted by the current model predicts the
349 field data more accurately although the difference between the three models is not very
350 significant, except at t >300 days. The dissipation of excess pore water pressure is very slow
351 and the remaining EPWP after 300 days is approximately 65 kPa. When the proposed model
352 is applied with a pre-consolidation pressure ratio (laboratory to field) of 0.79, the EPWP
353 dissipation curve with the current model represents a much closer comparison with field data
354 in relation to those by Yin and Graham (1989) and Indraratna and Redana (2000). The rate of
355 pore pressure dissipation is fastest for Indraratna and Redana (2000) followed by Yin and

356 Graham (1989). The current model predicts the slowest dissipation rate with a value of 55
357 kPa of undissipated EPWP after 300 days, compared to the measured value of 65 kPa in the
358 field.

359 **5. CONCLUSIONS:**

360 Although consolidation tests on small specimens under laboratory conditions can be used to
361 predict the field settlement well, it is often difficult to predict the dissipation of excess pore
362 water pressure over the long term. In order to make these predictions more accurate, in this
363 study, a radial consolidation model incorporating isotaches was proposed where the strain
364 rate dependency of pre-consolidation pressure was used to represent the in-situ strain rate.
365 The strain rate dependency can be calculated with the aid of constant rate of strain (CRS) plus
366 long term consolidation (LTC) laboratory testing. Once the pre-consolidation pressure
367 corresponding to the strain rate in the field is known, the change in effective stress due to
368 delayed consolidation ($\Delta\sigma_d'$) can be quantified with the associated EPWP dissipation rate.
369 Moreover, additional settlement can be also determined using the relevant coefficients of
370 secondary compression along with the strain rate.

371 The method of determining settlement and EPWP dissipation has been validated with three
372 different case histories (Ballina bypass, SBIA, Bangkok and Muar clay, Malaysia).
373 Conversion ratios of 0.86, 0.82, and 0.79 were used to transform laboratory pre-consolidation
374 pressure to the corresponding field consolidation pressure for Ballina, SBIA, and Muar clay,
375 with the results from this model showing good agreement with the field measurements. The
376 results from the current model were also compared with two previous models of Yin and
377 Graham (1989) and Indraratna and Redana (2005), demonstrating that a definite improvement
378 in prediction could be made using the current isotache model. This is possible as isotache
379 model involves the analysis based on field strain rate (model delayed consolidation) and

converts the laboratory pre-consolidation pressure into field pre-consolidation pressure using the factor obtained from well controlled CRS and LTC test data.

The pore water pressure at the Ballina site on the Pacific highway began to dissipate only after 250 days, even though settlement began earlier. While this could be attributed to some instrumental error, but with the Muar clay, the EPWP dissipation trends are very slow (similar to being without drains), however, the isotaches model somehow improved the prediction of pore water pressure dissipation compared to existing models.

The predictions from the proposed analytical model agree well with the laboratory and field results when incorporating the relationship between the pre-consolidation pressure and the strain rate (isotaches). The proposed solution in this study offers greater accuracy for predicting the settlement and excess pore water pressure, and this is validated through applications in 3 independent case histories, i.e. Pacific Highway (Ballina, NSW, Australia), Second Bangkok International Airport (Thailand) and North-South Expressway on Muar Clay (Malaysia). In particular, by incorporating the correct strain rate, the retarded dissipation of pore water pressure at the end of consolidation can be accurately quantified using the proposed method.

The findings of this study confirm that the strain rate effect is a key factor influencing the long term deformation and excess pore pressure dissipation occurring in soft clay foundations. The proposed approach is most beneficial in geotechnical practice where the long-term creep behaviour needs to be accounted for in visco-plastic soft clays.

6. ACKONWLEDGMENT

This research was supported by the Australian Government through an equivalent DECRA through the ARC Centre of Excellence in Geotechnical Science and Engineering (project CE110001009). The first author would like to thank the Australian Research Council (ARC)

Centre of Excellence in Geotechnical Science and Engineering (CGSE), Australian Research Council (ARC) Industrial Transformation Training Centre for Advanced Technologies in Rail Track Infrastructure (IC170100006), and the Centre for Geomechanics and Railway Engineering (CGRE), University of Wollongong for financial support during his PhD.

7. REFERENCES

Adachi, T., Oka, F. and Mimura, M. (1996). Modeling aspects associated with time dependent behavior of soils. Session on Measuring and Modeling Time Dependent Soil Behavior, ASCE Convention, Washington, Geot. Special Publication 61, 61–95.

AIT (1995). The full scale field test of prefabricated vertical drains for the Second Bangkok International Airport (SBIA). Final Report. Div. of Geotech. & Trans. Eng. AIT, Bangkok, Thailand.

Almeida, M.S.S., Santa Maria, P.E.L., Martins, I.S., Spotti, A.P. & Coelho, L.B.M. (2000) Consolidation of a very soft clay with vertical drains. Geotechnique, 50(2), 633-643.

Barden, L. (1969). Time dependent deformations of normally consolidated clays and peat. Journal of Soil Mechanics & Foundations Div. ASCE 95, SM 1, 1-31.

Barron R.A., (1948). Consolidation of fine-grained soils by drain wells. Trans. ASCE, 113, 718-754.

Bergado, D. T., Asakami, H., Alfaro, M.C., and Balasubramaniam, A.S. (1991). Smear effects of vertical drains in soft Bangkok clay. Journal of Geotechnical Engineering, ASCE, 117(10), 1509–1530.

427 Bergado, D.T., Balasubramaniam, A.S., Fannin, R.J. and Holtz, R.D. (2002). Prefabricated
428 vertical drains (PVDs) in soft Bangkok clay: A case study of the new Bangkok
429 International Airport project. Canadian Geotechnical Journal, 39, 304-315.

430 Bjerrum, L. (1967). Engineering geology of Norwegian normally-consolidated marine clays
431 as related to settlement of buildings. Géotechnique 17(2), 81-118.

432 Bo, M. W., Chu, J., Low, B. K. and Choa, V. (2003). Soil improvement; prefabricated
433 vertical drain techniques, Thomson Learning, Singapore.

434 Cao, L.F., Chang, M.F., The, C.I. & Na, Y.M. (2001). Back-calculation of consolidation
435 parameters from field measurements at a reclamation site. Canadian Geotechnical Journal,
436 38:755-769.

437 Chu, J. & Yan, S.W. (2005). Estimation of degree of consolidation for vacuum preloading
438 projects. International Journal of Geomechanics, 5(2): 158-165.

439 Geng X.Y., Indraratna B., and Rujikiatkamjorn C. (2012). Analytical Solutions for a Single
440 Vertical Drain with Vacuum and Time-Dependent Surcharge Preloading in Membrane and
441 Membraneless Systems. International Journal of Geomechanics, ASCE, 12(1), 27-42.

442 Hansbo, S. (1981). Consolidation of fine-grained soils by prefabricated drains and lime
443 column installation. In Proceedings of 10th International Conference on Soil Mechanics
444 and Foundation Engineering, Stockholm, A.A. Balkema, Rotterdam, The Netherlands. 3,
445 677-682.

446 Holtz, R.D., Jamiolkowski, M., Lancellotta, R. & Pedroni, S. (1991). Prefabricated Vertical
447 Drains: Design and Performance Heinemann-CIRIA, London.

448 Indraratna, B. and Redana, I. (2000). Numerical modeling of vertical drains with smear and
449 well resistance installed in soft clay. Canadian Geotechnical Journal, 37:132-145.

Indraratna, B., Rujikiatkamjorn, C., Kelly, R. B. & Buys, H. (2012). Soft soil foundation improved by vacuum and surcharge loading. Proceedings of the Institution of Civil Engineers: Ground Improvement, 165, 87-96.

Indraratna, B., Rujikiatkamjorn, C., Sathananthan, I., (2005). Analytical and numerical solutions for a single vertical drain including the effects of vacuum preloading. Canadian Geotechnical Journal, 43, 994–1014.

Indraratna, B., Baral, P., Rujikiatkamjorn, C. & Perera, D. (2018). Class A and C predictions for Ballina trial embankment with vertical drains using standard test data from industry and large diameter test specimens. Computer and Geotechnics, 93, 232-246.

Kelly, R. & Wong, P. K. (2009). An embankment constructed using vacuum consolidation. Australian Geomechanics, 44(2): 55-64.

Kim, Y.T. and Leroueil, S. (2001). Modelling the viscoplastic behaviour of clays during consolidation: application to Berthierville clay in both laboratory and field conditions. Canadian Geotechnical Journal, 38(3), 484–497.

Kjellman, W. (1952). Consolidation of clayey soils by atmospheric pressure. Proceedings of a conference on soil stabilization, Massachusetts Institute of Technology, Boston, 258-263.

Kobayashi, M., Furudoi, T., Suzuki, S. and Watabe, Y. (2005). Modelling of consolidation characteristics of clays for settlement prediction of Kansai International Airport, Proc. Symp. Geotech. Aspects Kansai Int. Airport, 65-76.

Ladd, C. C. (1973). Estimating settlement of structures supported on cohesive soils. Special summer program, 1.34s, Massachusetts Institute of technology, Cambridge.

Leroueil, S. (2006). The isotache approach-Where are we 50 years after its development by Professor Suklje?. Proc., 13th Danube-European Conf. on Geotechnical Engineering, Slovenian Geotechnical Society, Ljubljana, Slovenia: 55-58.

474 Leroueil, S., Kabbaj, M. and Tavenas, F. (1988). Study of the validity of a σ'_v–σ_v– model in
475 in situ conditions. Soils and Foundations, 28(3), 3–25.

476 Mesri, G. and Castro, A. (1987). The Cα/Cc concept and K0 during secondary compression.
477 Journal of Geotechnical Engineering, ASCE, 113(3), 230–247.

478 Ratanayake, A.M.P. (1991). Performance of test embankment with and without vertical
479 drains at Muar Clays, Malaysia, AIT M Eng. thesis, Bangkok, Thailand.

480 Rujikiatkamjorn, C., Indraratna, B. and Chu, J. (2008). 2D and 3D Numerical modelling of
481 combined surcharge and vacuum preloading with vertical drains, International Journal of
482 Geomechanics, 8(2):144-156

483 Suklje, L. (1957). The analysis of the consolidation process of the isotache method.
484 Proceedings, 4th International conference on Soil Mechanics and Foundation Engineering,
485 London 1, 200-206.

486 Tanaka, H., Udaka, K. and Nosaka, T. (2006). Strain rate dependency of cohesive soils in
487 consolidation settlement. Soils and Foundations, 46(3), 315–322.

488 Tang, X.W., Onitsuka, K. (2001). Consolidation of double-layered ground with vertical
489 drains. International Journal for Numerical and Analytical Methods in Geomechanics. 25,
490 1449–1465.

491 Tsusumi, A. and Tanaka, H. (2011).Compressive behavior during the transition of strain rate.
492 Soils and Foundations, 51(5): 813–822.

493 Walker, R., and Indraratna, B. (2009). Consolidation analysis of a stratified soil with vertical
494 and horizontal drainage using the spectral method. Géotechnique 59, 439–449.

495 Watabe, Y. and Leroueil, S. (2015). Modelling and implementation of the isotache concept
496 for long-term consolidation behavior. Int. J. for Geomechanics, 15, A4014006-1.

497 Watabe, Y., Udaka, K., Nakatani, Y. & Leroueil, S. (2012). Long-term consolidation
498 behaviour interpreted with isotache consept for worldwide clays. Soils and Foundations,
499 52, 449-464.

500 Yang, C., Carter, J.P., Sheng, D. & Sloan, S. (2016). An isotach elastoplastic constitutive
501 model for natural soft clays. Computers and Geotechnics, 77: 134-155.

502 Yin, J.H. and Graham, J. (1989). Viscous-elastic-plastic modelling of the time-dependent
503 stress-strain behaviour of clays. Canadian Geotechnical Journal, 31: 42-52.

504

505

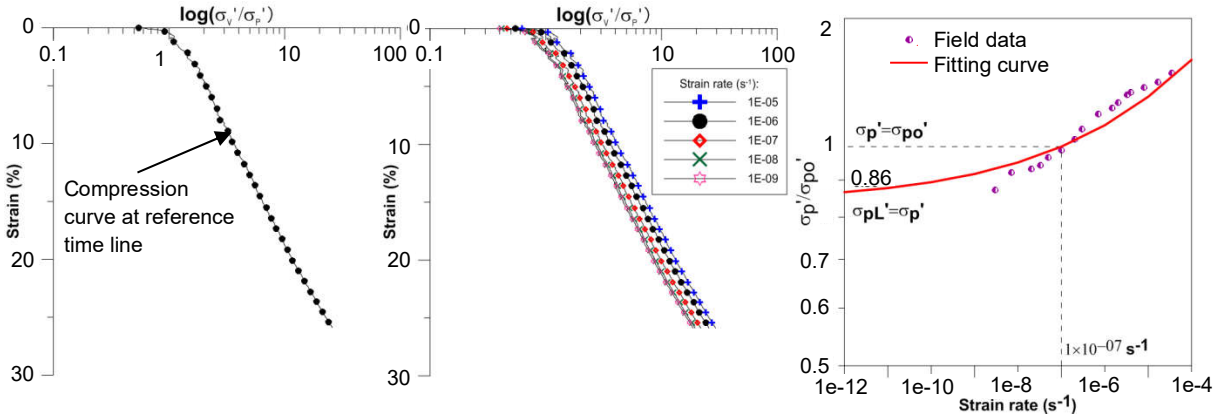

(a) (b) (c)

Figure 2: Illustration of the method used to determine the strain rate dependency of pre-consolidation pressure with a constant rate of strain (CRS) and long term (LTC) consolidation test, (a) Reference time line, (b) Isotaches for Ballina clay, (c) Strain rate dependency of pre-consolidation pressure.

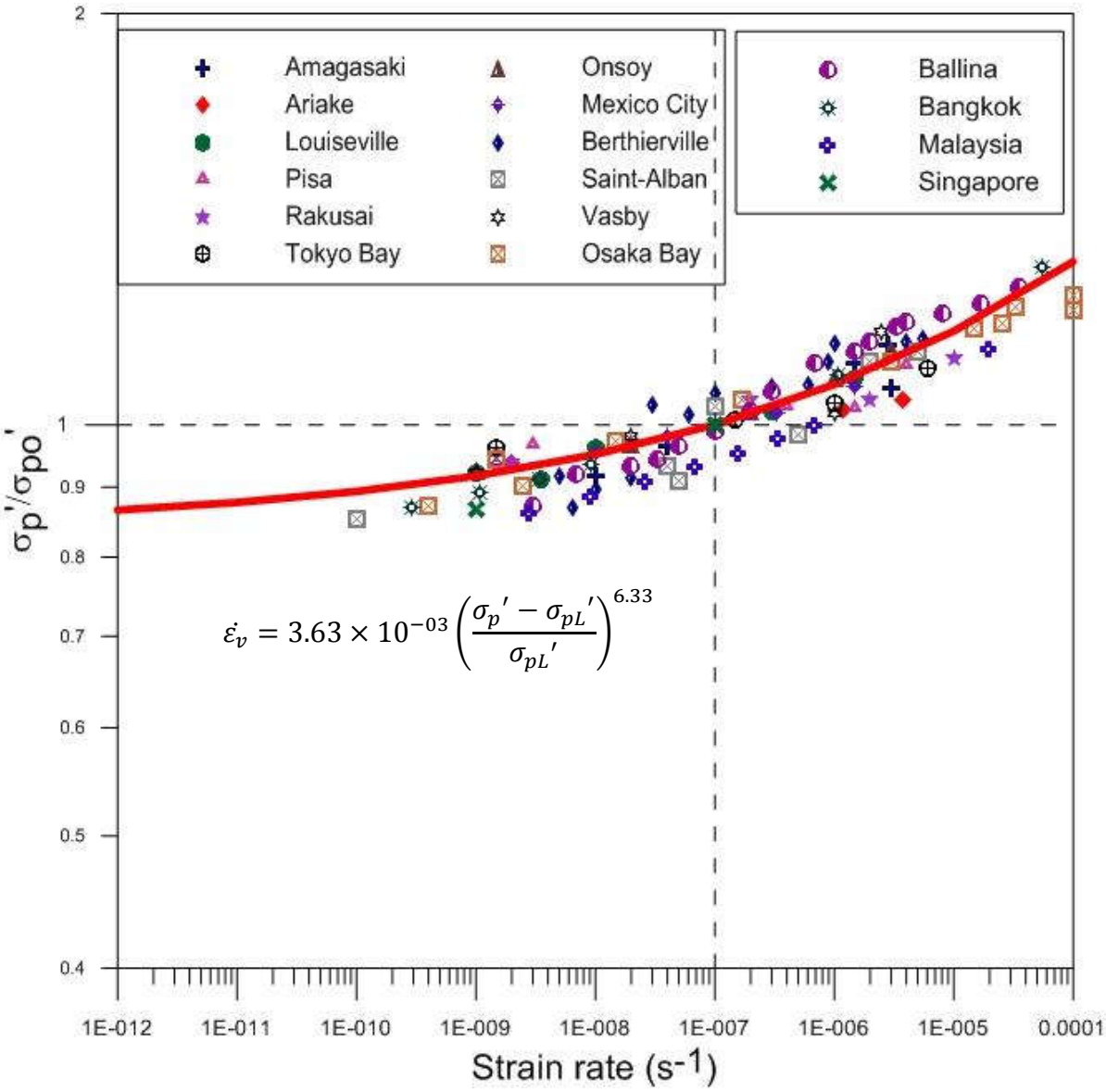

Figure 3: Log ($\frac{\sigma_p{}'}{\sigma_{p0}{}'}$)-log strain rate ($\dot{\varepsilon_v}$) curve for all the worldwide clays by Watabe and Leroueil (2015), including clays obtained from Ballina, Bangkok, Malaysia and Singapore.

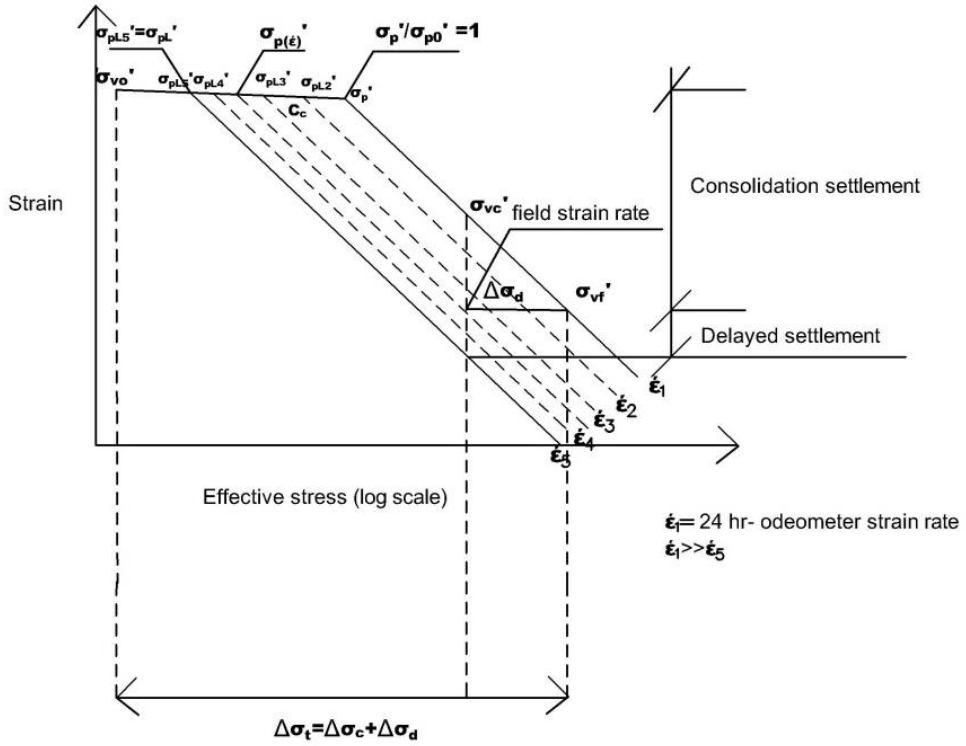

Figure 4: Conceptual model considering the isotaches approach

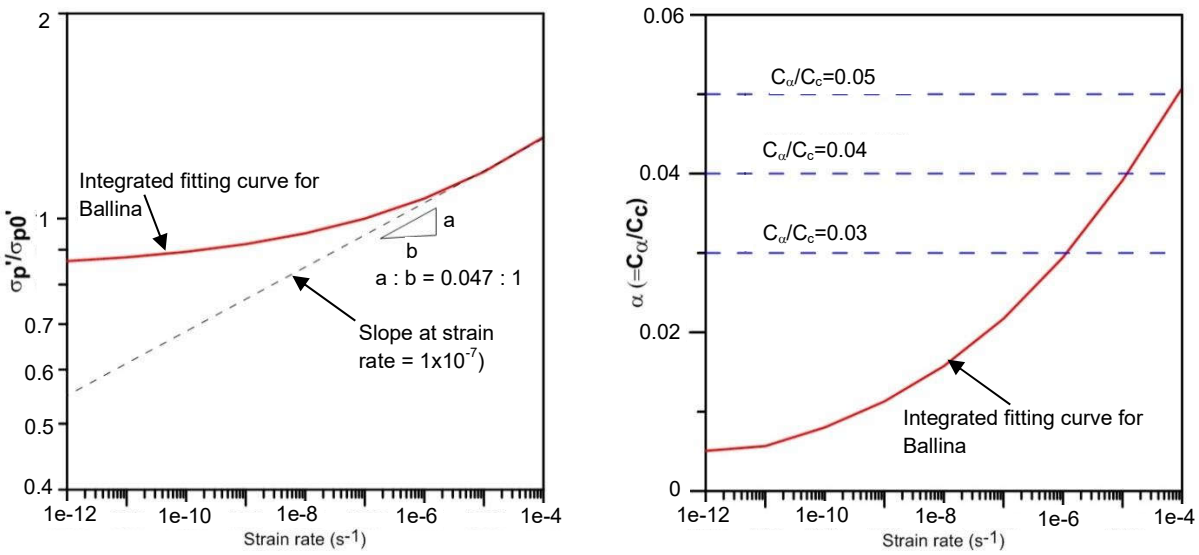

(a) (b)

Figure 5: Comparison of integrated fitting curve with Mesri and Castro (1987), C_α/C_c concept, (a) strain rate dependency curve with slope, (b) relationship between strain rate and $\alpha(=C_\alpha/C_c)$

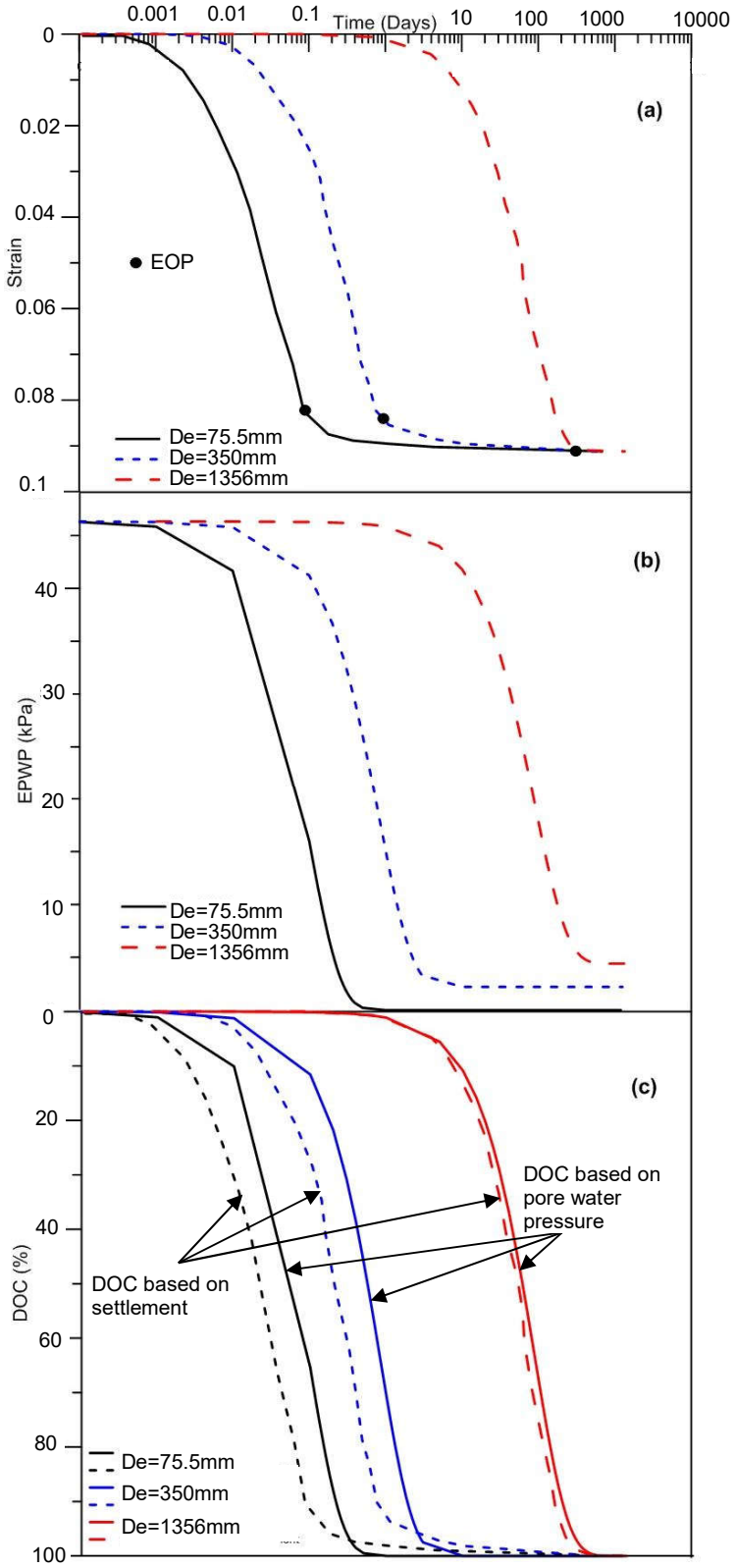

Figure 6 (a) Time-strain curve for specimens with different drainage path, (b) Excess pore water pressure (EPWP) dissipation of specimens with different drainage path & (C) DOC based on settlement and pore water pressure for three different specimens

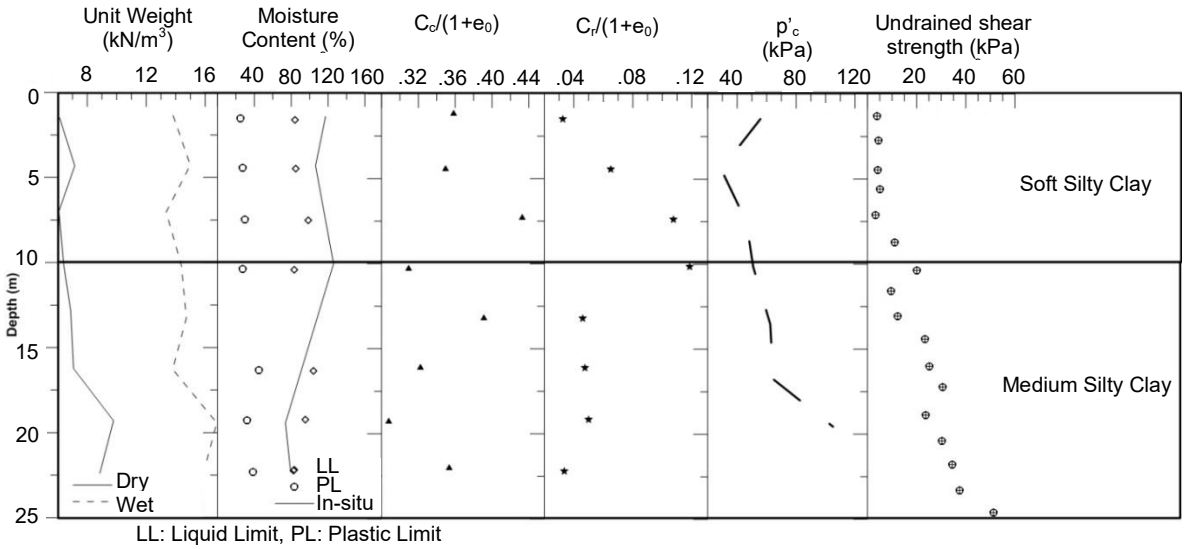

Figure 7: Basic soil properties of Ballina bypass

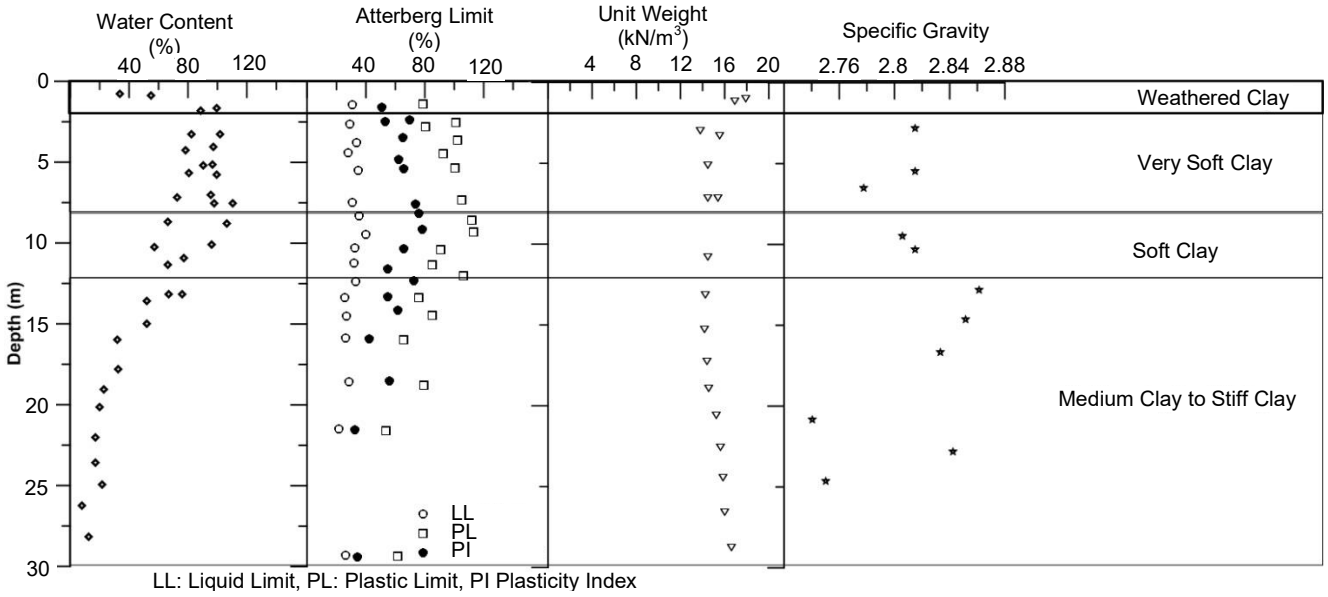

Figure 9: Soil characteristics of SBIA.

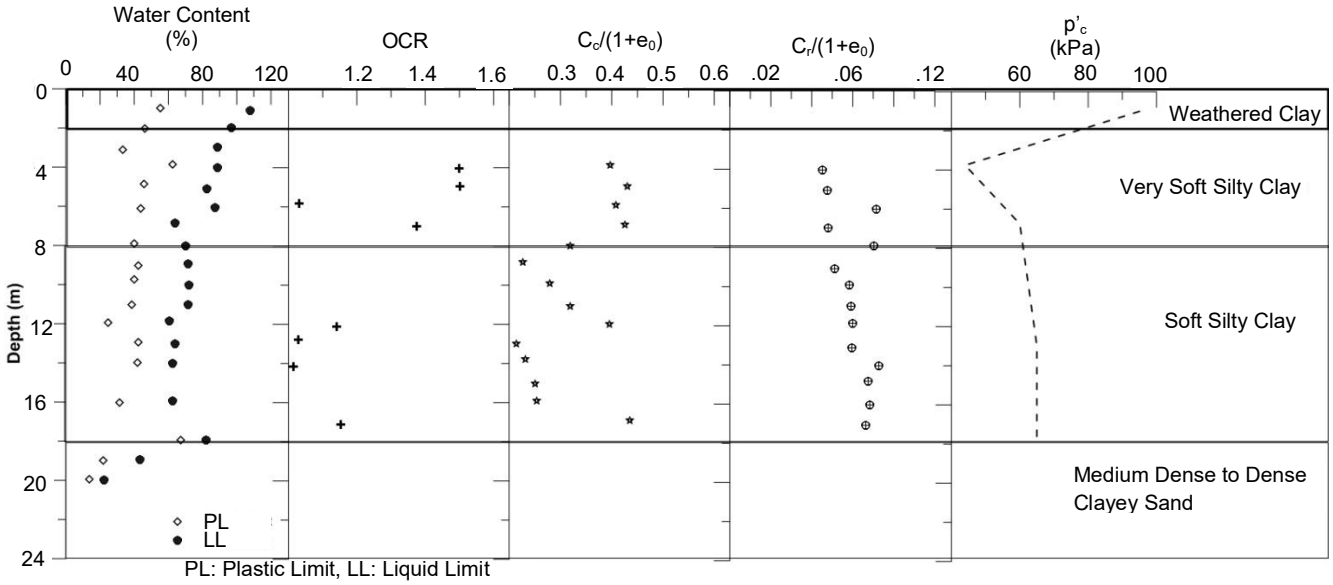

Figure 14: Sub-soil properties of Muar clay.